[

Low-Co rare-earth-based hydrogen storage alloy①

LI Quan-an(李全安), SANG Ge(桑 革), LI Jian-wen(李建文),
CHEN Yun-gui(陈云贵), TU Ming-jing(涂铭旌), LI Ning(李 宁)
(Department of Metal Materials, Sichuan University, Chengdu 610065, P.R.China)

[Abstract] On the basis of typical high-Co MI(Lanthanum-rich mischmetal)-based hydrogen storage alloy, a series of low-Co or Co-free alloys have been prepared by means of partial or full replacement of Co by a combination of other elements. The microstructures, *p-c-T* (pressure-concentration-temperature) characteristics and electrochemical properties under different charge-discharge conditions of the alloys have been investigated. Compared with the high-Co alloy, the low-Co or Co-free alloys have the lower hydrogen equilibrium pressure and discharge capacity, but have the nearly same high-rate and high temperature discharge capability, and better charge-discharge cycling stability. The reason is revealed by SEM, XPS and XRD results.

[Key words] low-Co hydrogen storage alloy; metal hydride electrode; rare-earth alloy; electrochemical property; Ni-MH battery

[CLC number] TG139⁺.7 **[Document code]** A

1 INTRODUCTION

The rare-earth-based AB_5-type alloys have been investigated extensively as electrode materials. The typical compositions of commercial AB_5-type alloys are $MmNi_{3.55}Co_{0.75}Mn_{0.4}Al_{0.3}$ and $MINi_{3.55}Co_{0.75}Mn_{0.4}Al_{0.3}$ (MI: Lanthanum-rich mischmetal, Mm: Cerium-rich mischmetal). It is well known that cobalt is a key alloying element and has been proved to have a positive effect on the charge-discharge cycling stability of the AB_5-type alloy[1,2]. However, cobalt is the most expensive component in the rare earth-based AB_5-type alloy. The currently commercial AB_5-type alloy usually contains about 10% (mass fraction) Co. According to average market price, cobalt takes up 40% ~ 50% share of the total raw material cost of the alloy. In order to enhance the marketability of Ni-MH(metal hydride) batteries and further apply Ni-MH battery to electric vehicles in future, the low cost AB_5-type alloy and cheap Ni-MH battery must be available. Therefore, intensive attempts to develop low-Co and Co-free AB_5-type alloy with new chemical composition are ongoing at many laboratories around the world[3~9].

A series of multi-component low-Co and Co-free AB_5-type alloys have been designed according to the alloying principle of AB_5-type alloys as electrode materials[10]. The microstructures, electrochemical properties and *p-c-T* characteristics of the alloys, and composition distribution in surface layer of alloy electrodes have been investigated.

2 EXPERIMENTAL

The alloy compositions examined in this work are listed in Table 1. The alloys were melt in a vacuum induction furnace under an argon atmosphere, and then were cooled by copper mould. Lanthanum-rich mischmetal MI is our patent composition. The as-cast alloys were crushed and ground mechanically, then passed through a series of sieves. The fine power with a size of less than 38 μm was used for X-ray power diffraction (XRD) measurements. The power with size of 38 ~ 75 μm was used for electrochemical measurements.

Electrochemical properties of MH electrodes were tested in a half-cell (in 6 mol/L KOH electrolyte at 20 ℃ and 40 ℃) with a computer-controlled current source. The MH electrodes were fabricated by mixing the alloy power (approximately 200 mg) with the fine copper in a mass ratio of 1 : 2, followed by cold pressing on a pellet (d = 10 mm, p = 2.55 × 10^9 Pa). A $Ni(OH)_2$ electrode (sintered) with a larger capacity and a Hg/HgO(6 mol/L KOH) electrode were used as the counter-electrode and reference electrode, respectively. Electrodes were charged at 0.2, 0.4 and 1 C rate for 7.5, 3.5 and 1.3 h respectively, and discharged at the same rate to a cut off potential of -0.600 V vs the Hg/HgO(6 mol/L KOH) electrode.

The microstructure analysis of the alloys was carried out using scanning electron microscopy (SEM) and energy dispersive X-ray analysis (EDX). The phase structure and the lattice constants of the alloys were determined using XRD.

The *p-c-T* curves of the alloys were measured at 20 ℃ and 40 ℃ by electrochemical method. The enthalpy and entropy changes of hydrogen desorption were obtained via the Van't Hoff equation.

①[Received date] 1999-03-26; [Accepted date] 1999-06-12

Table 1 Lattice parameters and electrochemical properties of alloys at 0.4 C charge-discharge rate

Alloy	Alloy composition	Lattice constant		Cell volume	x(Co)	Capacity Q	Capacity decay
		a/Å	c/Å	/Å^3	/%	/(mAh·g^{-1})	/%
6-1	$MlNi_{3.55}Co_{0.75}Al_{0.3}Mn_{0.4}$	5.037 (4.936)*	4.032 (4.306)	88.554 (90.876)	0.75	322	31.4
3-1	$MlNi_{3.55}Co_{0.60}Al_{0.3}Mn_{0.40}Cu_{0.15}$	5.044 (4.936)	4.035 (4.326)	88.912 (91.294)	0.6	309	31.6
3-6	$MlNi_{3.40}Co_{0.50}Al_{0.3}Mn_{0.35}Cu_{0.25}Fe_{0.1}Si_{0.1}$	5.049 (4.949)	4.046 (4.331)	89.353 (91.879)	0.5	304	25.0
3-2	$MlNi_{3.55}Co_{0.40}Al_{0.3}Mn_{0.40}Cu_{0.15}Fe_{0.1}Si_{0.1}$	–	–	–	0.4	299	27.8
3-5	$MlNi_{3.40}Co_{0.30}Al_{0.3}Mn_{0.35}Cu_{0.30}Fe_{0.1}Si_{0.1}Cr_{0.15}$	–	–	–	0.3	273	26.6
3-9	$MlNi_{3.50}Co_{0.30}Al_{0.3}Mn_{0.35}Cu_{0.30}Fe_{0.00}Si_{0.1}Cr_{0.15}$	–	–	–	0.3	269	32.0
3-3	$MlNi_{3.55}Co_{0.20}Al_{0.3}Mn_{0.40}Cu_{0.15}Fe_{0.10}Si_{0.10}Cr_{0.20}$	–	–	–	0.2	268	29.4
3-4	$MlNi_{3.55}Co_{0.00}Al_{0.3}Mn_{0.40}Cu_{0.40}Fe_{0.10}Si_{0.1}Cr_{0.15}$	–	–	–	0	248	25.8

* The data in brackets got from the specimen after 280 charge-discharge cycles at 0.4 C rate

their chemical states in the surface layer of alloy electrodes after 280 charge-discharge cycles at 0.4 ℃ rate were analyzed by X-ray photoelectron spectroscopy (XPS) using Mg K_a radiation of energy 1253.6 eV.

3 RESULTS AND DISCUSSION

3.1 X-ray diffraction

The XRD results indicated that all alloys examined in this work seems to be single phase with the hexagonal $CaCu_5$-type crystal structure. The lattice constants (a, c) and unit volume of three representative alloys are summarized in Table 1. Partial replacement of Co by Cu or by a combination of Cu, Fe and Si lead to a lattice expansion. After 280 charge discharge cycles, the alloys are still hexagonal $CaCu_5$-type crystal structure, but a axis decreases, c axis increases, axis ratio c/a becomes larger. Anisotropic expansion is generally observed in replaced $LaNi_5$ alloys, which have a larger axis ratio c/a. This is due to the occupation by H of the site near the $Z = 1/2$ plane[11]. It was also found that after 280 charge-discharge cycles, the X-ray diffraction peak broadens, which is attributed to the lattice distortion and grain refining in charge-discharge process.

3.2 Electrochemical properties

3.2.1 discharge capacity and cycling stability

The discharge capacities of the alloys are also listed in Table 1. Partial (or full) replacement of Co by a combination of Cu, Fe, Si and Cr causes a relatively large decrease of discharge capacity, while partial replacement of Co by Cu or by a combination of Cu, Fe and Si (Co content 0.4-0.75) only causes a slight decrease of discharge capacity.

Fig. 1 shows the relationships between discharge capacity and cycle number for the four representative alloys. It can be seen from Fig. 1 and Table 1 that the cycling stability for low-Co alloys except for alloys 3-1 and 3-9 is higher than that for high-Co alloy 6-1, especially alloys 3-6, 3-2 and 3-5 (partial replacement of Co by a combination of Cu, Fe and Si, Co content 0.3 ~ 0.5) have not only the satisfactory cycling stability but also the rather high discharge capacities. For alloy 3-4, although it has quite satisfactory cycling stability, it is not suitable for electrode materials because of its too low discharge capacity. For alloy 3-1, the low cycling stability is due to the partial replacement of Co by only one element Cu, whereas the replacement of Co by a combination of multi-component has more positive effect on cycling stability. For alloy 3-9, the low cycling stability is due to that it is Fe-free, whereas Fe has the same positive effect as Co on improving of cycling stability. Apart from the positive effect of Fe on cycling stability, the reasons why the low-Co alloys show high cycling stability could be explained by the following factors. Firstly, small amounts of silicon in the AB_5-type alloy can improve the cycling stability since silicon forms a tight surface oxide layer which effectively protects the inner alloy from further oxidation[12,13]. Secondly, according to a neutron diffraction investigation[14], 50% of Cu atoms in Cu-containing AB_5-type alloys can occupy the 2 C Ni-site (plane $Z = 0$), Cu behaves in somewhat similar way to Co, and the replacement of the components in side B by Cu lowers the Vickers hardness. A reduced hardness could improve the cycling stability[15]. Thirdly, it was reported that Cr-containing AB_5-type alloys also could improve the cycling stability[16]. Finally, EDX analysis showed that the

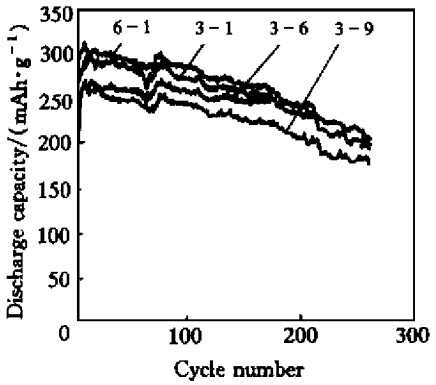

Fig.1 Discharge capacity vs cycle number for four representative alloy electrodes (Charge at 0.4 C rate for 3.5 h; Discharge at 0.4 C rate to cut-off potential −0.6 V vs Hg/HgO)

secondary phase in grain boundary is predominantly rich in Cr (67%, mole fraction) with small amounts of Ni, Cu and Mn. However, the secondary phase can not be detected by XRD because of its limited quantity, as shown in Fig.2. The function of the secondary phase is to form micro-encapsulation of grain, which could further improve cycling stability for low-Co alloys[7].

3.2.2 High-rate discharge capability

Discharge capabilities at various rates at 20 ℃ is showed in Table 2 and Fig. 3.

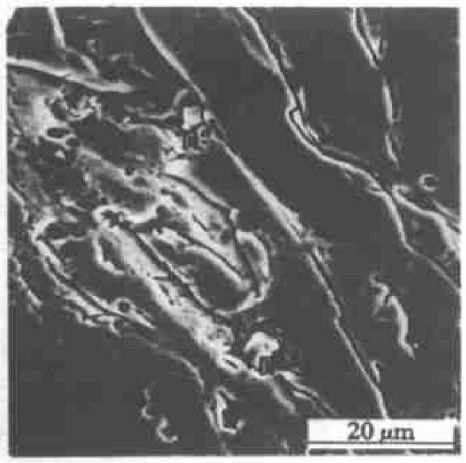

Fig.2 SEM image of as-cast alloy

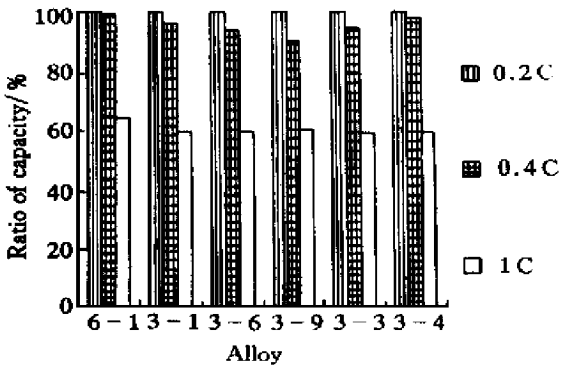

Fig.3 Discharge properties at various charge-discharge rates at 20 ℃

As shown from Table 2 and Fig.3, the discharge capacity at 20 ℃ decreases with the increase of discharge rate, but for all alloy examined in this work the ratios of the discharge capacity at the same charge-discharge rate (1 C or 0.4 C rate) to that at 0.2C rate are nearly a same value, which indicates that decreasing cobalt content by means of partial replacement Co by multi-component could not only improve charge-discharge cycling stability, but also keep high-rate discharge capability basically unchanged. The high-Co alloy 6-1 (with Co 0.75) has the best high-rate discharge property, which could be explained by the fact that Co can give the oxidized alloy surface a good electronic conductivity by a dissolution precipitation process because cobalt hydroxide has good electronic conductivity[17], therefore, the high Co alloy facilitates the improvement of high-rate discharge capability. The results of electrochemical impedance spectroscopy (EIS) further proved that the high-Co alloy has the smallest charge-transfer resistance[7], so the alloy 6-1 has the best hydriding-dehydriding kinetics property and high-rate discharge capability.

3.2.3 Discharge capacity at various temperatures

Discharge capacities at various temperatures at 0.2 C charge-discharge rate are listed in Table 2. Discharge capacity at 40 ℃, compared with that at 20 ℃, only decreases slightly, and for all alloys the

Table 2 Discharge capacities under various charge-discharge conditions

Alloy	Alloy compositions	x(Co)/%	20 ℃, 0.2 C capacity /(mAh·g^{-1})	20 ℃, 0.4 C capacity /(mAh·g^{-1})	20 ℃, 1 C capacity /(mAh·g^{-1})	40 ℃, 0.2 C capacity /(mAh·g^{-1})
6-1	$MlNi_{3.55}Co_{0.75}Al_{0.3}Mn_{0.4}$	0.75	325	322	210	301
3-1	$MlNi_{3.55}Co_{0.60}Al_{0.3}Mn_{0.40}Cu_{0.15}$	0.6	323	309	192	295
3-6	$MlNi_{3.40}Co_{0.50}Al_{0.3}Mn_{0.35}Cu_{0.25}Fe_{0.1}Si_{0.1}$	0.5	325	304	192	274
3-9	$MlNi_{3.50}Co_{0.30}Al_{0.3}Mn_{0.35}Cu_{0.30}Fe_{0.00}Si_{0.1}Cr_{0.15}$	0.3	298	269	181	261
3-3	$MlNi_{3.55}Co_{0.20}Al_{0.3}Mn_{0.40}Cu_{0.15}Fe_{0.10}Si_{0.10}Cr_{0.20}$	0.2	283	268	167	260
3-4	$MlNi_{3.55}Co_{0.00}Al_{0.3}Mn_{0.40}Cu_{0.40}Fe_{0.10}Si_{0.1}Cr_{0.15}$	0	254	248	154	254

ratios of those are in the range of 84.3 %- 99.6 %, and the ratios for all alloys except for the alloy 3-6 are more than 90 %, which indicates that discharge capacity of the alloys studied in this work is hardly affected by temperature in the range of 20 ~ 40 ℃. The reason why discharge capacity of the alloy 3-6 is sensitive to temperature is that this alloy contained relatively much of Cu but no Cr, Cu enhance the sensitiviy to temperature whereas Cr can suppress the sensitivity.

Increasing temperature has two respects of effect on discharge capacity: increasing temperature could generally make discharge capacity increase. On the other hand, too high temperature could make discharge capacity decrease, which can be explained by following facts.

1) The charge-discharge process is, in fact, a hydriding-dehydriding process. The dehydriding process is an endothermic reaction. According to reaction kinetics theory, an increase of temperature facilitates endothermic reaction, so higher temperature is favorable to discharge.

2) According to Van' t Hoff equation, $\lg p = \Delta H/RT - \Delta S/T$, equilibrium hydrogen pressure p increases with the increasing of temperature, which increase discharge potential, e.g. dehydriding is easy and the hydrogen is easily oxidized to water at higher temperature. So discharge capacity increases with the increasing of temperature, especially at high rate. Even at still higher temperature, there is a tendency that discharge capacity at large current is higher than that at small current, which is ascribed to the decreasing of charge-transfer resistance with the increasing of temperature[18] besides the hydrogen pressure affection.

3) However when temperature is too high, the diffusive speed of hydrogen in alloy increases rapidly, and then a part of hydrogen diffusing to alloy surface has no time to be oxidized to water due to the limited surface electrocatalysis and so forms H2, which not only decreases charge efficient, but also increases self-discharge rate. So discharge capacity decreases at too high temperature.

As analyzed above, rational composition design can obtain the less sensitive alloy to temperature in a wider temperature range.

3.3 *p-c-T* characteristics

The *p-c-T* curves of four representative alloys are showed in Fig.4, and the midpoint pressures of plateau region in *p-c-T* curve are summarized in Table 3. The alloy 6-1 with cobalt content 0.75 had the widest plateau region and relatively high plateau pressure. With the decreasing of cobalt content and the addition of other alloying elements, plateau becomes shorter and plateau pressure be lowered, but plateau slope be varied slightly. The addition of alloying elements such as Mn, Al, Cr, Si, Fe, Cu could lower the plateau pressure of alloy hydride because they can increase unit volume. Decreasing plateau pressure could suppress pulverization and then improve charge-discharge cycling stability. The lower the hydrogen equilibrium pressure, the more stable the alloy hydride, then electrode polarization increases during discharging, which lowers the discharge efficiency. So all of the low-Co or Co-free alloys examined in this work had higher cycling stability, but their discharge capacities decrease more or less because of their lower equilibrium pressures.

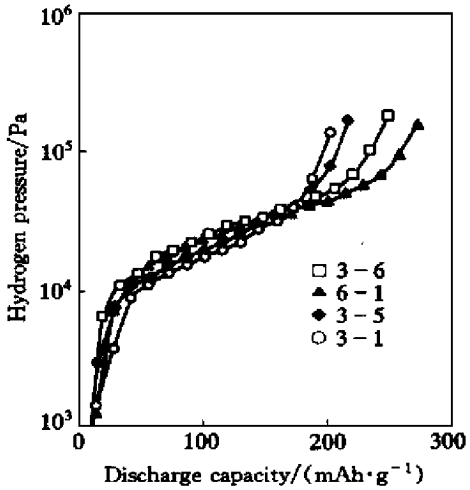

Fig. 4 *p-c-T* curves of four representative alloys at 40 ℃

Table 3 Hydrogen equilibrium pressure, ΔH and ΔS

Alloy	Equilibrium pressure /10^4 Pa		ΔH /(kJ·mol^{-1})	ΔS /(kJ·mol^{-1}·K^{-1})
	20 ℃	40 ℃		
6-1	1.711	2.746	−77.3043	−0.20096
3-1	2.329	3.344	−59.0346	−0.15652
3-6	2.030	3.129	−70.6485	−0.18434
3-2	1.774	2.740	−71.0448	−0.18088
3-5	1.652	2.246	−50.1567	−0.10706
3-9	1.652	2.405	−61.3479	−0.14526
3-3	1.258	1.844	−62.5259	−0.13957
3-4	1.542	2.102	−50.5476	−0.10594

According to Van' t Hoff equation, enthalpy and entropy changes of alloy hydride were obtained using plateau pressures at 20 ℃ and at 40 ℃ and the results are also listed in Table 3. It can be seen that the hydriding reaction heat (- ΔH) of the alloys is in between 50 ~ 78 kJ/mol. Among the 8 alloys, the heat for alloy 6-1 is largest. According to thermodynamics theory, the larger the reaction heat, the more the hydrogen absorbs, and then, the higher discharge capacity the alloy may has.

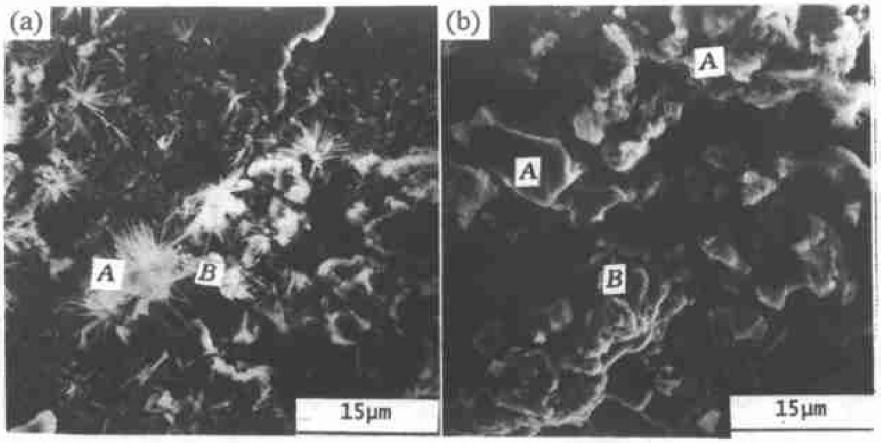

Fig.5 SEM images of electrode surface
(a)—Alloy 6-1, containing Co 0.75(mole fraction, %); (b)—Alloy 3-1, containing Co 0.6(mole fraction, %)

3.4 Surface analysis of alloy electrodes

The results of SEM analysis for alloy electrodes show that with the decreasing of cobalt content and the addition of other alloying elements, the amount of oxide covering electrode surface decreases, and then alloy particles and their pulverization behavior could be observed clearly, as shown in Fig.5, which indicates that partial replacement of cobalt by multi-component could greatly improve the antioxidation ability of the alloys.

The results of XPS analysis of electrode surface for alloys 6-1 and 3-6 indicate that after 280 cycles at 0.4C charge-discharge rate, there are large amounts of Al(50 % ~ 90 %, mole fraction) and Si(10 % ~ 18 %) in surface layer which existed in the state of Al_2O_3 and Si_2O_3 respectively. It suggests that the Al and Si added to alloy have formed tight surface oxide layer, which have protects the inner alloy from further oxidation. Co was found as $Co(OH)_2$ only within 300 Å depth. $Co(OH)_2$ can facilitate improvement of discharge capacity and high-rate charging and discharging because it has a good electronic conductivity[17]. The concentrations of Ni and La at electrode surface are lowered to 8.6 % ~ 30 % and 2.0 % ~ 4.0 % respectively, which exists in the states of Ni_2O_3, $La(OH)_3$ and La_2O_3, and enriches to surface. And within 2 000 Å depth Ni and La have been fully oxidized after 280 charge-discharge cycles then dissolved from the surface, which causes the concentrations of Ni and La much lower than their bulk concentrations. It is just the oxidization and the loss of active material that make discharge capacity decrease continuously. Mn was not found in the analysis depth range (2000 Å), which is due to that the concentration of Mn at surface is too low to be detected by XPS because of its strong tendency to dissolution from the surface during charge-discharge cycling. With regard to Fe, maybe the amount of its addition to alloy and enrichment at surface was too small to be detected. With regard to Cu, its concentration in alloy could not be determined because electrodes contained large amounts of Cu power as compacting material.

4 CONCLUSIONS

1) Partial replacement of Co by a combination of multi-components causes the decrease of discharge capacity more or less, but improves the cycling stability.

Partial replacement Co down to 0.4 from 0.75 (mole fraction, %) by Cu or by a combination of Cu, Fe and Si only causes a slight decrease of discharge capacity, but obviously improves the cycling stability.

Full replacement of Co by Cu, Fe, Si and Cr gets a satisfactory cycling stability, but causes a too much decrease of discharge capacity.

2) The low-Co (or Co-free) alloy possesses the nearly same high temperature discharge capacity and high-rate discharge capability as the high-Co alloy.

3) The low-Co or Co-free alloy has a lower plateau pressure, but the plateau slope varies slightly.

Decreasing of the Co content of AB5-type alloy according to multi-component alloying principle causes the decrease of discharge capacity more or less, but it could obviously improve cycling stability and keep the high-rate discharge capability and the high temperature discharge capability basically unchanged, which shows it is promising to develop low-Co and Co-free hydrogen storage alloy as electrode material.

[REFERENCES]

[1] Sakai T, Oguro K, Miyamura H, et al. Some facts affecting the cycle lives of LaNi5-based alloy electrodes of hydrogen battery [J]. J Less-Common Met, 1990, 161: 193-202.

[2] Willems J J G. Metal hydride stability of $LaNi_5$-related compounds [J]. Philips J Res, 1984, 39(Suool.1): 1.

[3] PAN Hong-ge. Influence of Co content on kinetic properties of $MINi_{4.3-x}Co_xAl_{0.7}$ hydrogen storage alloys [J]. The Chinese Journal of Nonferrous Metals, (in Chinese), 1999, 9(3): 453 - 457.

[4] Yashda K. Effects of the materials processing on the hydrogen absorption of $MmNi_5$-type alloys [J]. J Alloys Comp, 1997, 253/254: 621 - 625.

[5] Higashiyama N, Matsuura Y, Nakamura H, et al. Influence of preparation methods of non-stoichiometric hydrogen-absorbing alloys on the performance of nickel-metal hydride secondary batteries [J]. J Alloys Comp, 1997, 253/254: 648 - 651.

[6] Hu W K. Effect of microstructure, composition and non-stoichiometry on electrochemical properties of low-Co rare-earth nickel hydrogen storage alloys [J]. J Alloys Comp, 1998, 279: 295- 300.

[7] Hu W K, Lee H, Kim K M, et al. Electrochemical behaviors of low Co Mm-based alloys as MH electrodes [J]. J Alloys Comp, 1998, 268: 261 - 265.

[8] Hu W K, Kim D M and Jang K J. Study on Co-free rare earth based hydrogen storage alloys [J]. J Alloys Comp, 1998, 269: 254 - 253.

[9] Lichtenberg G, Köhler U, Fölzer A, et al. Development of AB5 type hydrogen storage alloys with low Co content for rechargeable Ni-MH batteries with respect to electric vehicle applications [J]. J Alloys Comp, 1997, 253/254: 570 - 573.

[10] LI Quan-an, CHEN Yun-gui, TU Ming-jing, et al. The properties of electrode and the design of chemical composition of AB_5-type hydrogen storage alloy [J]. Chinese Journal of Power Sources, (in Chinese), 2000, 24(4): 246 - 250.

[11] Nakamura Y, Sato K, Fujitani S, et al. Lattice expanding behavior and degradation of $LaNi_5$-based alloys [J]. J Alloys Comp, 1998, 267: 205 - 210.

[12] Willems J J G and Buschow K H J. From permanent magnets to rechargeable hydride electrices [J]. J Less-common Metals, 1987, 129: 13 - 30.

[13] Meli F, Zuttel A and Schlaphach L. Surface and bulk properties of alloys from the viewpoint of battery applications [J]. J Alloys Comp, 1992, 190: 17 - 24.

[14] Percheron-Guegan A, Lartigue C and Achard J C. Correlation between the structural properties, the stability and the hydrogen content of substituted $LaNi_5$ compounds [J]. J Less-Common Metals, 1985, 109: 287-309.

[15] chartouni D, Meli F, Zuttel A, et al. The influence of Co on the electrochemical cycling stability of $LaNi_5$ based hydride forming alloy [J]. J Alloys Comp, 1996, 241: 160 - 166.

[16] Sakai T, Miyamura H, Kuriyama N, et al. Some factors affecting the cycle lives of $LaNi_5$-based alloy electrodes of hydrogen battery [J]. J Less-Common Metals, 1990, 161: 127 - 139.

[17] Oshitani M, Yufu H, Takashima S, et al. Development of a pasted nickel electrode with high active material utilization [J]. J Electrochem Soc, 1989, 136: 1590-1593.

[18] Hu W K, Kim D M, Jeon S W, et al. Effect of annealing treatment on electrochemical properties of Mmbased hydrogen storage alloys for Ni/MH batteries [J]. J Alloys Comp, 1998, 270: 255 - 264.

(Edited by ZHU Zhong-guo)